

# Photoinduced Harpoon Reactions as a Probe of Condensed-Phase Dynamics: ICI in Liquid and Solid Xenon

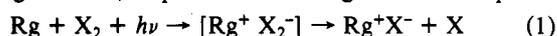
F. Okada,<sup>†</sup> L. Wiedeman, and V. A. Apkarian\*

Department of Chemistry, University of California, Irvine, California 92717 (Received: May 11, 1988; In Final Form: July 7, 1988)

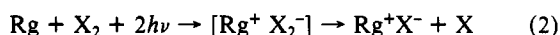
Two-photon-induced harpoon reactions of ICI in liquid and solid xenon are reported. The reaction dynamics is followed by monitoring the luminescent products: the triatomic Xe<sub>2</sub>Cl and Xe<sub>2</sub>I exciplexes. Action spectra and branching ratios as a function of excitation energy are reported. The efficient production of the nonthermodynamic product, the iodide, in the liquid phase implies that the cage exit of the ejected Cl atom is direct and sudden. The absence of iodide in the crystalline solids establishes the absence of direct cage exit in the ordered phase. Line-shift measurements at the phase transition indicate that the exciplexes are strongly clustered in the liquid phase. The effect of clustering on dynamics is the prevention of exchange between iodide and chlorine—the solvent cage excludes Cl atoms. Branching ratios and action spectra are used to identify the potential surfaces in the exit channel and the optical resonances in the entrance channel. The two-photon charge-transfer excitations are enhanced by two-electron resonances that allow selectivity of products.

## Introduction

Photoinduced harpoon reactions between molecular halogens and rare-gas atoms, to produce the rare-gas halide exciplexes



proceed efficiently in condensed media, in both solid<sup>1-3</sup> and liquid<sup>4-6</sup> rare gases. While the optical threshold of these processes is in the UV,<sup>6</sup> the cross sections are large enough to induce them via two-photon laser excitation:<sup>1-5</sup>



These reactions were among the earliest examples advanced for the study of gas-phase reactions induced by radiation resonant with intermolecular potentials—an example of the general class of radiative collisions.<sup>7,8</sup> As such, both the one-photon<sup>7-11</sup> and two-photon<sup>12-14</sup> versions have been characterized in the gas phase. The latter, the two-photon-induced harpoon reaction, has also been recently studied in Rg:X<sub>2</sub> van der Waals complexes generated in molecular beams.<sup>15,16</sup> There are direct analogies between the elementary photophysics of these processes in complexes isolated in the gas phase or solvated by a liquid or solid host. The differences are due to many-body contributions, the central issue in condensed-phase dynamics which we intend to probe in these studies.

The inordinate efficiency of these reactions in condensed phases has led to the postulation of a “negative” cage effect (dissociation facilitated by cage atoms),<sup>3,5</sup> and the proposition of the two-photon harpoon reaction as a general pumping scheme for liquid-phase rare-gas halide exciplex lasers.<sup>6</sup> The studies of ICI in both liquid and solid xenon, which will be reported here, were designed to test and establish the methodology of photoinduced harpooning as a technique for unraveling condensed-phase dynamics and energetics. The chemical pertinence of ionic reactions in condensed phases is obvious; it may also be argued that the liquid phase is the more natural medium for harpooning. We anticipate these studies to play a role in establishing microscopic relations between energetics and dynamics in dense media, similar to the role played by classical harpoon reactions in advancing gas-phase molecular dynamics.

## Experimental Section

The experiments are conducted in a high-pressure cryocell. An early design of such a cell, a two-window cell, has previously been presented.<sup>4</sup> Several improvements on the design of the cell have occurred during the course of these studies. A three-window T-cell, suitable for fluorescence studies, was constructed with OFHC

copper. The cell was electroplated with gold and attached to an all-Monel gas-handling manifold. A closed-cycle cryostat (CTI C22) is used for cooling. Temperature measurement and control are provided by a diode sensor and a 25-W resistive heater. A major improvement in this system is its long-term temperature stability—the temperature could be maintained within 0.1 K of a preset value over time periods longer than 16 h.

A temperature gradient is established in the cell by point-heating it at the gas inlet. Transparent solids could be reproducibly prepared in these cells by slow growth. This is achieved by maintaining the cell temperature, with temperature gradient in place, constant within 0.1 K of the freezing point of the solution and allowing the solid to grow across the gradient. These optically nonscattering solids will grow to fill the entire cell (a cylinder of 1.25-cm diameter and 4-cm length) over the period of 10–16 h. The possibility of zone refining during the slow growth of the crystalline solid from ICI:Xe solutions is suspected but not verified.

An excimer-pumped dye laser equipped with doubling crystals (Lambda Physik EMG 201 MSC/FL 3002) was used for these studies. The emission spectra were recorded with a 0.25-m polychromator and an optical multichannel analyzer with a diode array of 990 active elements (EG&G OMA III). Lifetimes were measured with either a boxcar averager (SRS) or a 150-MHz

- (1) Fajardo, M. E.; Apkarian, V. A. *J. Chem. Phys.* **1986**, *85*, 5660.
- (2) Fajardo, M. E.; Apkarian, V. A. *Chem. Phys. Lett.* **1987**, *134*, 51.
- (3) Fajardo, M. E.; Apkarian, V. A. *J. Chem. Phys.* **1988**, *89*, 4102.
- (4) Wiedeman, L.; Fajardo, M. E.; Apkarian, V. A. *Chem. Phys. Lett.* **1987**, *134*, 55. Fajardo, M. E.; Wiedeman, L.; Apkarian, V. A. *Proceedings of IQEC*, PD-16, Baltimore, 1987.
- (5) Fajardo, M. E.; Withnall, R.; Feld, J.; Okada, F.; Lawrence, W.; Wiedeman, L.; Apkarian, V. A. *Laser Chem.* **1988**, *9*, 1.
- (6) Fajardo, M. E.; Apkarian, V. A.; Moustakas, A.; Krueger, H.; Weitz, E. *J. Phys. Chem.* **1988**, *92*, 357.
- (7) Yakovlenko, S. I. *Sov. J. Quantum Electron.* **1978**, *8*, 151.
- (8) Dubov, V. A.; Gudzenko, L. I.; Gurvich, L. V.; Iakovlenko, S. I. *Chem. Phys. Lett.* **1977**, *45*, 330; **1977**, *46*, 25.
- (9) Grieneissen, H. P.; Xue-Jing, Hu; Kompa, K. L. *Chem. Phys. Lett.* **1981**, *82*, 421.
- (10) Dubov, V. S.; Lapsker, Ya. E.; Samoilova, A. N.; Gurvich, L. V. *Chem. Phys. Lett.* **1981**, *83*, 518.
- (11) Wilcomb, B. E.; Burnham, R. *J. Chem. Phys.* **1981**, *74*, 6784.
- (12) Yu, Y. C.; Setser, D. W.; Horiguchi, H. *J. Phys. Chem.* **1983**, *87*, 2209.
- (13) Ku, J. K.; Inoue, G.; Setser, D. W. *J. Phys. Chem.* **1983**, *87*, 2989.
- (14) Setser, D. W.; Ku, J. K. In *Photophysics and Photochemistry Above 6 eV*; Elsevier: New York, 1985; p 621.
- (15) Boivineau, M.; LeCalve, J.; Castex, M. C.; Jouvot, C. *Chem. Phys. Lett.* **1986**, *128*, 528; *J. Chem. Phys.* **1986**, *84*, 4712.
- (16) Jouvot, C.; Boivineau, M.; Duval, M. C.; Soep, B. *J. Phys. Chem.* **1987**, *91*, 5416.

<sup>†</sup>Permanent address: Central Research Laboratory, Nippon Mining Co., 3-17-35 Niizo-Minami Toda-Shi, Saitama, Japan.

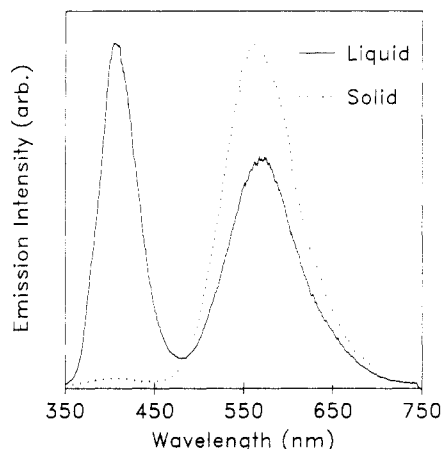


**Figure 1.** Emission spectra at the freezing point of ICl/Xe solutions. The liquid-phase emission (dashed line) shows both  $\text{Xe}_2\text{I}$  and  $\text{Xe}_2\text{Cl}$  emissions with nearly equal intensities. The solid-phase spectrum (solid line) is from a crystalline sample—the iodide emission is nearly absent. The spectra were recorded by two-photon excitation at 308 nm of a 0.25 mM solution.

digitizing/averaging scope (Tektronix 2430).

Xenon of 99.999% purity was purchased (Spectra Gases) and used without further purification. ICl was transferred to a blackened glass bulb equipped with a greaseless Teflon stopcock. It was used after several freeze-pump-thaw cycles and always transferred from an ice/water bath to avoid  $\text{I}_2$  contamination. The vapor pressure (22 Torr at room temperature) was always measured prior to transfer as a check for the absence of contamination by  $\text{Cl}_2$ . The experiments are conducted in fresh ICl/Xe samples. Samples that are kept overnight or that have been extensively irradiated invariably undergo some disproportionation. In all of the experiments reported here, the cryocell was first filled with  $\sim 5$  Torr of ICl—measured in the room-temperature manifold—and transferred to the cell held at  $\sim 180$  K. Sufficient xenon is subsequently added to fill the entire cell with liquid.

## Results

Two-photon laser excitation of ICl:Xe solutions in the near UV produces emission from both iodide and chloride exciplexes of xenon. In solid or liquid xenon, only the lowest energy exciplexes, namely,  $\text{Xe}_2^+\text{I}^-(4^2\Gamma)$  and  $\text{Xe}_2^+\text{Cl}^-(4^2\Gamma)$ , are observed.<sup>5</sup> A liquid-phase emission spectrum obtained by 308-nm excitation of a 0.25 mM solution in equilibrium with the solid (at the freezing point of Xe of 161.25 K) is shown in Figure 1. Both iodide and chloride emissions are prominent at 400 and 562 nm, respectively. A solid-state emission spectrum, obtained from the same sample under identical conditions except upon completion of freezing, is also shown in the same figure. The interrogated volume of the solid in this case was optically nonscattering—visually clear. Both emission intensities and line centers of these bands undergo abrupt changes upon phase transition—the iodide emission nearly disappears in the crystalline solid, and both emission line centers undergo a blue-shift by  $\sim 5$  nm. This abrupt change is only observed in solids of high optical quality, obtained by slow freezing of the solution. In frosty, amorphous solids obtained by fast freezing, the line shift is negligible, and the relative intensity of the iodide and chloride emissions varies depending on the particular volume of interrogation in a given solid. The temperature dependence of chloride and iodide emissions, near the freezing point of xenon, at 165 K, is shown in Figure 2. There clearly is a dramatic difference between emission line centers in crystalline versus amorphous solids. While this effect is always observed, the extent of the blue-shift upon freezing is not exactly reproducible—the solid-state emission suffers from inhomogeneous contributions that cannot be well quantified due to the broad nature of these exciplexic bound-free emissions.

That the exciplexes are produced by two-photon excitation is verified by fluence-dependence studies. Log-log plots of emission intensity versus excitation fluence are illustrated in Figure 3.

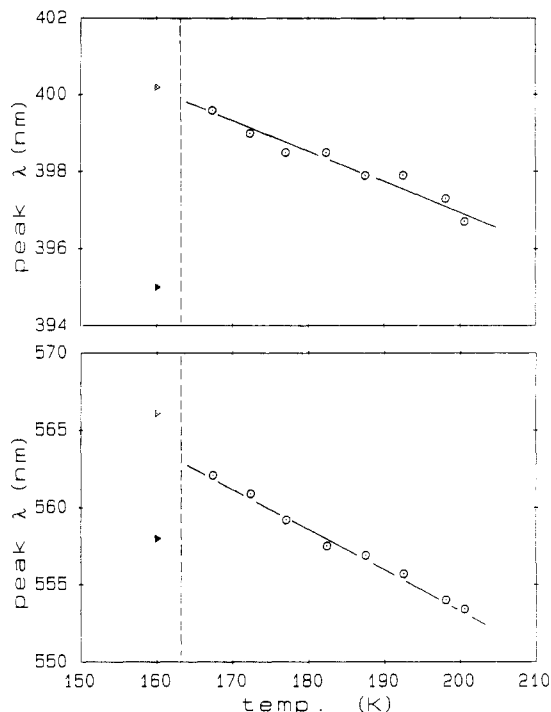


**Figure 2.** Emission maxima  $\text{Xe}_2^+\text{I}^-$  (top panel) and  $\text{Xe}_2^+\text{Cl}^-$  (bottom panel) versus temperature. The dashed line represents the melting point of the solid. The open circles represent liquid-phase data, the open triangle is that of an amorphous solid obtained by supercooling of the solution, while the filled triangle represents emission maxima obtained from crystalline xenon.

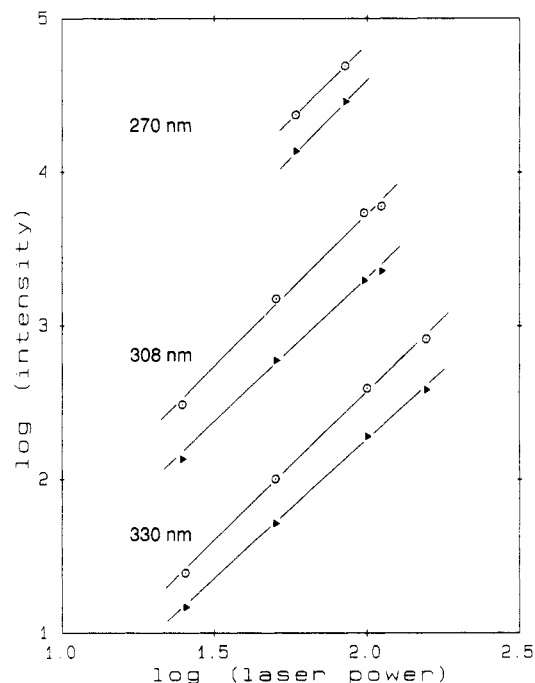


**Figure 3.** Power dependence of  $\text{Xe}_2\text{I}$  (open circles) and  $\text{Xe}_2\text{Cl}$  (filled triangles) at the indicated excitation wavelengths. The ordinate is in arbitrary units; the data have been vertically displaced for better visibility. At all studied wavelengths, the power dependence is within  $1.96 \pm 0.1$ .

Similar results are obtained at selected wavelengths in the studied spectral range of 265–365 nm. The slopes of the log-log plots in all cases lie within  $1.96 \pm 0.10$ , clearly indicating the two-photon nature of the excitation process.

The exciplexes could be produced throughout the studied excitation range. Due to the nonlinearity of the photogeneration process, the most reliable action spectra (product emission intensity as a function of reagent excitation wavelength) are obtained by maintaining the laser fluence—energy and beam profile—constant.

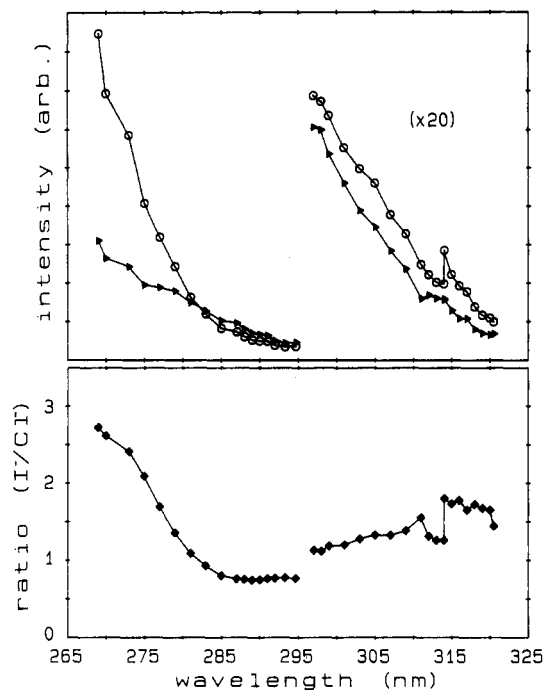


**Figure 4.** Top: liquid-phase action spectra obtained at 165 K by monitoring  $\text{Xe}_2^+\text{I}^-$  emission at 400 nm (open circles) and  $\text{Xe}_2^+\text{Cl}^-$  emission at 560 nm (filled triangles). Bottom: product branching ratio,  $\gamma$ , defined in eq 3, as a function of excitation wavelength. The arrow shows the two-photon thermodynamic threshold for production of the iodide.

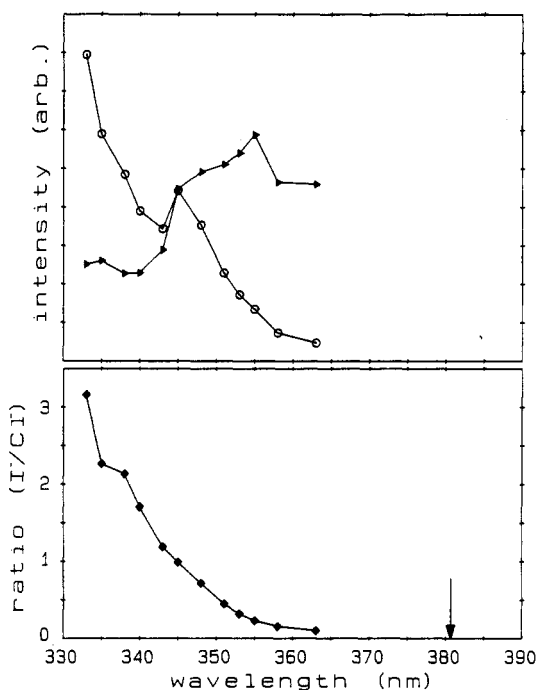


**Figure 5.** Same as in Figure 4. In the excitation spectra the data in the 300–320-nm range have been multiplied by a factor of 20.

This was achieved by using an attenuator (Newport Corp. 935-3) external to the laser and by recording spectra at discrete wavelength intervals over the gain curve of the given dye. Two different spectral ranges were studied: the threshold region, the spectral range between 330 and 365 nm, was studied by using a single dye, and the spectral range between 265 and 325 nm was studied by using three overlapping dyes and a KDP doubling crystal. The action spectra obtained by monitoring the  $\text{Xe}_2^+\text{Cl}^-$  and  $\text{Xe}_2^+\text{I}^-$  are illustrated in the top panels of Figures 4 and 5.

The time evolution of the two emissions, in liquid xenon, is illustrated in Figure 6. In the liquid phase, just above the melting point of xenon, both iodide and chloride relax exponentially with

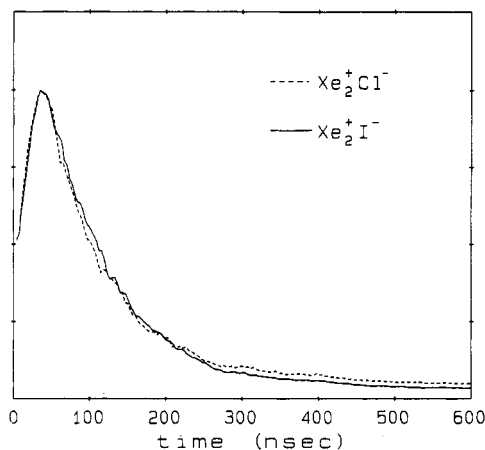


**Figure 6.** Fluorescence decay of  $\text{Xe}_2\text{I}^-$  (dashed line) and  $\text{Xe}_2\text{Cl}^-$  (solid line) in liquid xenon. Both emissions are well fit with an exponential of  $100 \pm 7$  ns lifetime.

identical lifetimes. The observed liquid-phase lifetimes depend on temperature and initial ICl concentration much as in the case of  $\text{Cl}_2/\text{Xe}$  solutions discussed previously.<sup>17</sup> There, it was shown that the exciplex relaxation time was determined by diffusion-controlled encounters between the exciplex and parent molecular halogen. The relaxation times in the examples of Figure 6 are  $100 (\pm 7)$  ns. Upon freezing the solution and therefore eliminating diffusion, the  $\text{Xe}_2^+\text{Cl}^-$  relaxes strictly by radiation,  $\tau = 245 (\pm 15)$  ns. The  $\text{Xe}_2^+\text{I}^-$  emission clearly shows a double-exponential decay: a fast part that follows the laser pulse, and a long tail that decays with the radiative lifetime of  $138 (\pm 9)$  ns. The radiative lifetimes obtained from 12 K matrix measurements are  $225 (\pm 10)$  and  $130 (\pm 12)$  ns for  $\text{Xe}_2^+\text{Cl}^-$  and  $\text{Xe}_2^+\text{I}^-$ , respectively.<sup>3</sup>

Given the fact that the observed decay for both exciplexes is the same in the liquid phase, the absolute branching ratio,  $\gamma = \text{Xe}_2^+\text{I}^-/\text{Xe}_2^+\text{Cl}^-$ , can be obtained from the integrated emission spectra as

$$\gamma = \left[ \frac{\int I(\omega) d\omega}{\tau_r} \right]_{\text{Xe}_2^+\text{I}^-} \left[ \frac{\tau_r}{\int I(\omega) d\omega} \right]_{\text{Xe}_2^+\text{Cl}^-} \quad (3)$$

Since the iodide and chloride emissions have the same fluence dependence, the branching ratio need not be corrected for laser characteristics (beam profile, pulse shape or energy). The branching ratio obtained from different measurements, at similar concentrations and temperatures, are plotted in the lower panels of Figures 4 and 5 as a function of excitation wavelength. No corrections were made for instrumental response.

In the crystalline solids prepared by slow freezing of solutions,  $\gamma \sim 0.05$  and is independent of excitation wavelength throughout the studied spectral range of 334–365 nm. In amorphous solids a great variability in branching ratios is observed depending on the particular volume probed.

## Discussion

**Spectral Shifts. Clustering and the Solvent Shield Effect.** The gas-phase emission spectra of the triatomic exciplexes is well-known: the  $\text{Xe}_2\text{I}(4^2\Gamma)$  emission is centered near 375 nm while the  $\text{Xe}_2\text{Cl}(4^2\Gamma)$  emission is centered near 485 nm.<sup>18</sup> The emission spectra of all the xenon halides isolated in xenon matrices have previously been reported and discussed: the  $\text{Xe}_2\text{I}$  and  $\text{Xe}_2\text{Cl}$  emissions are centered near 390 and 573 nm in 12 K matrices.<sup>3</sup> Liquid-phase emission spectra of selected exciplexes have also been reported.<sup>19</sup> The large shifts of the exciplexic emissions upon

(17) Wiedeman, L.; Fajardo, M. E.; Apkarian, V. A. *J. Phys. Chem.* **1988**, *92*, 342.

(18) *Excimer Lasers*, Rhodes, C. K. Ed.; Topics in Applied Physics; Springer-Verlag: New York, 1984; Vol. 30.

(19) Jara, H.; Pummer, H.; Egger, H.; Rhodes, C. K. *Phys. Rev. B: Condens. Matter* **1984**, *30*, 1.

condensation is due to the ionic-covalent nature of the transitions involved and the large dipole of the emitting state. The dependence of the emission on the density of the medium, and hence bulk polarizability, has been documented in some detail in the case of  $\text{Xe}_2^+\text{Cl}^-$  in gaseous, liquid, and solid xenon.<sup>17</sup> That the emission is sensitive to the structure of the host is obvious from the abrupt blue-shift that accompanies the phase transition, as illustrated in Figure 2. This dramatic behavior has been documented in the case of  $\text{Xe}_2\text{I}$  generated in HI/Xe solutions.<sup>20</sup> In that case solids of high spectral quality could be prepared by slow freezing and could be maintained without damage down to temperatures as low as 25 K. It was established there, that the  $\text{Xe}_2\text{I}$  emission undergoes (a) a gradual red-shift of  $\sim 5$  nm in the liquid phase, in the temperature range between 210 and 161 K, (b) an abrupt, 10-nm blue-shift upon crystallization at constant temperature, at the freezing point of the liquid, and (c) a gradual blue-shift of  $\sim 5$  nm in the transparent solid, between 161 and 25 K. Clearly, the abrupt blue-shift observed upon slow freezing of the solutions is related to the establishment of crystalline order. This is further verified by the observation that in frosty, optically scattering solids obtained by supercooling the solutions, the discontinuity in the line shifts is absent, see Figure 2.

While the discontinuity of the line shift upon freezing implies the establishment of crystalline order, its sign, the blue-shift, implies the reduction of the local xenon density around the immediate vicinity of the exciplex. This conclusion can easily be reached by considering the classical solvent shift models,<sup>21</sup> which have previously been demonstrated to adequately account for both solid-<sup>1,3</sup> and liquid-<sup>17</sup> phase line shifts of the exciplexes. According to the Onsager cavity model, the line shift is proportional to  $\mu^2/d^3$ , where  $\mu$  is the transition dipole of the solute and  $d$  is the diameter of the isolation cavity.<sup>21,22</sup> Thus a blue-shift implies an increase in  $d$  upon crystallization, i.e., the  $\text{Xe}_2^+\text{X}^-$ -Xe nearest-neighbor distance is smaller in the liquid phase than in the solid phase. This in turn implies that the local solvent density in the liquid phase is larger than that of the crystalline solid and therefore much larger than the bulk density of the liquid. In short, the exciplex is extensively clustered in liquid xenon.

This conclusion is perhaps not too surprising. The photogeneration of the exciplex in liquid xenon corresponds to the instantaneous creation of a large dipole in a polarizable medium. Note that the emission spectra are collected on the relaxation time scale ( $\sim 10^{-7}$  s), a time scale long enough to allow the complete relaxation of the solvent around the dipole. Thus a collapse of the solvent cage atoms around the dipole due to dipole-induced dipole attractions is to be expected. In the liquid phase, this attractive force is balanced by the repulsive wall of the van der Waals potentials. In the crystalline solid, the optimal geometry around the dipole is to be compromised due to the cohesive energy of the crystal. Note that the latter is only operative in the presence of long-range order and hence implies that the exciplexes are isolated in crystalline environments even though the macroscopic solid is most likely to be polycrystalline.

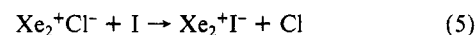
While the picture of a caged dipole in the liquid-phase rationalizes the line-shift data, its consideration is essential for the interpretation of the relaxation dynamics. In detailed concentration and temperature dependence studies of  $\text{Xe}_2^+\text{Cl}^-$ , it was established that the liquid-phase deactivation is due to diffusion-controlled encounters with the parent molecular halogen— $\text{Cl}_2$  in those studies.<sup>17</sup> Nevertheless, the deactivation probability was estimated to be  $\sim 0.1$  per encounter, while in the gas phase the deactivation rate due to the same process is gas kinetic.<sup>9,23,24</sup> This reduced deactivation efficiency and the saturation effect in line shifts were taken as hints of clustering. Yet the conjecture could not be affirmed, since the arguments were based on estimates of

diffusion rates and concentrations, both of which are subject to uncertainties.<sup>17</sup> In the present experiments, it is the absence of back reaction between the iodide exciplex and chlorine that clearly forces the conclusion that the exciplex is caged and that the solvent cage protects it from attack by Cl atoms.

The argument is as follows. The exchange reaction



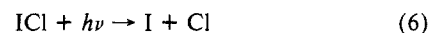
is exoergic by  $\sim 0.9$  eV in liquid xenon. This can be estimated from the emission spectra alone. Since the iodide is created from ICl, there necessarily is a geminately created Cl atom in the vicinity of the exciplex. Thus, in the absence of special considerations, the exchange reaction is to be expected to proceed on a time scale much shorter than the laser pulse width of  $\sim 17$  ns used in these experiments, and hence the survival of any iodide emission would be unexpected. Not only is the iodide emission intensity larger than the chloride emission throughout most of the studied spectral region, but also the fluorescence lifetimes of the two exciplexes are identical in the liquid phase as illustrated in Figure 6. The implication of the latter observation is that both exciplexes relax with the same rate-determining step. In the case of  $\text{Xe}_2^+\text{Cl}^-$ , it has previously been established that neither Cl nor Xe is effective in relaxing the exciplex.<sup>17</sup> Moreover, the exchange reaction



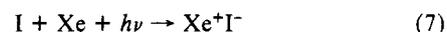
is endoergic and therefore unlikely. Thus it is possible to conclude that  $\text{Xe}_2^+\text{Cl}^-$  is quenched by diffusion-controlled encounters with ICl and therefore the same is true about  $\text{Xe}_2^+\text{I}^-$ . Moreover, we are forced to conclude that the back reaction (eq 4) is blocked in the liquid phase. The only plausible explanation is one of a tight cage formed around the exciplex, a cage that excludes all Cl atoms. Since the atomic polarizability of Cl is nearly half that of xenon, its exclusion from a cage constructed by dipole-induced forces is reasonable. Evidently the cage is effective in shielding the exciplex from any back reaction with atoms; however, diatomics such as  $\text{Cl}_2$  and ICl remain effective in quenching the exciplexes.

**Cage Exit Dynamics.** The solvent shield effect discussed in the previous section was based on the observation of the persistence of the iodide emission. The efficient photoproduction of the iodide from ICl in liquid xenon is not a trivially obvious result in view of the thermodynamic stability of the chloride. Here we consider the implication of its efficient production and the observed branching ratios as a function of excitation energy.

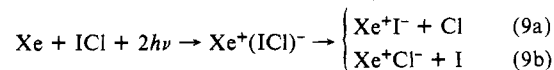
First, it is important to note that the possible mechanism of photodissociation and subsequent photoassociation:



followed by



can be discarded as a significant channel for the two-photon production of the exciplexes in the present experiments. The optical thresholds for the charge-transfer reactions of eq 7 and 8 have been measured in solid xenon doped with atomic halogens to be 280 and 360 nm, respectively.<sup>3</sup> While ICl possesses continuous dissociative absorptions in the entire UV-vis spectral range<sup>25</sup> and hence the sequential mechanism for the production of xenon chloride, eq 6 followed by eq 8, is possible, this mechanism could not explain the prominence of the iodide in the 280–360-nm range. It is then clear that the photoproduction of exciplexes proceeds via the ionic potentials accessed by two-photon-induced harpooning between xenon and ICl:



(20) Lawrence, W.; Okada, F.; Apkarian, V. A. *Chem. Phys. Lett.* **1988**, *150*, 339.

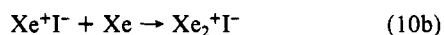
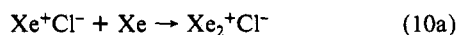
(21) McKean, D. C. *Spectrochim. Acta* **1967**, *A23*, 2405.

(22) Onsager, L. *J. Am. Chem. Soc.* **1936**, *58*, 1486.

(23) McCown, A. W.; Eden, J. G. *J. Chem. Phys.* **1984**, *81*, 2933.

(24) Marowsky, G.; Sauerbrey, R.; Tittel, F. K.; Wilson, W. L. *Chem. Phys. Lett.* **1983**, *98*, 167.

The possible optical resonances in the entrance channel of this harpoon reaction will be discussed below. Here we consider the implications of the observed branching ratios. Note that since the reactions are conducted in xenon as the solvent, only the triatomic exciplexes are observed. The reactive quenching of diatomics to form the triatomics:



is known to proceed on a picosecond time scale in both solid<sup>1,3</sup> and liquid<sup>17</sup> solutions of xenon. Thus the ratio of triatomic emission intensities represents the nascent exciplexic branching ratio of eq 9.

The efficient photoproduction of the iodide from ICl in liquid xenon has significant implications in view of the thermodynamic stability of the chloride. The thermodynamic thresholds,  $E_{\text{th}}$ , for the production of a given exciplex is given, according to eq 9, as

$$E_{\text{th}} = D_0(\text{ICl}) + E(\text{Xe}^+\text{X}^-) \quad (11)$$

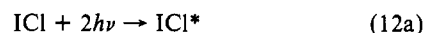
in which  $D_0$  is the dissociation energy of ICl, 2.15 eV, and  $E(\text{Xe}^+\text{X}^-)$  is the minimum of interionic potential relative to the unbound neutral ground state. The latter is well approximated by the observed excitation thresholds in I:Xe and Cl:Xe solids—3.55 eV for  $E(\text{Xe}^+\text{Cl}^-)$  and 4.35 eV for  $E(\text{Xe}^+\text{I}^-)$ . Thus independent of the exact mechanism in the photoproduction of the charge-transfer complex,  $\text{Xe}^+(\text{ICl})^-$ , if the solvent cage moderates the ejection of the neutral halogen atom in eq 9, i.e., if the ejected atoms suffer collisions prior to cage exit, then we would expect the reaction to proceed via the lowest energy path. This path would clearly correspond to the production of the chloride (i.e., eq 9b) based on the thermodynamic thresholds given above. Therefore, sudden cage exit of Cl atoms is a precondition for the production of  $\text{Xe}_2^+\text{I}^-$ . However, note that cage exit of the neutral iodine atom is not essential for the production of  $\text{Xe}_2^+\text{Cl}^-$  since the back reaction of iodine with the chloride, eq 5, is prohibitively endoergic. The photoproduction of the iodide in liquid xenon is kinetically possible only at excitation energies that exceed  $E_{\text{th}}(\text{Xe}^+\text{I}^-)$  by an increment that corresponds to the cage barrier for sudden exit of Cl. It can clearly be seen in Figure 4 that as the excitation energy nears the thermodynamic threshold of exciplex production the  $\text{I}^-/\text{Cl}^-$  branching ratio nears zero while the chloride emission intensity remains constant. If we assume that the entire excess energy is in the form of Cl + I relative kinetic energy, then from the appearance energy of the iodide emission,  $\sim 6.95$  eV, it can be inferred that sudden cage exit of the Cl atom is possible even at an excess energy of only  $\sim 0.45$  eV. Below this limit, direct cage exit is not possible, and the system will follow the lower energy channel, i.e., the production of  $\text{Xe}_2^+\text{Cl}^-$ .

These arguments are most clearly supported by the dramatic change in branching ratios that accompanies phase transitions. It can be deduced from Figure 1 that upon creation of a crystalline solid, direct cage exit is virtually impossible. The iodide emission nearly disappears. The observed broad residual emission can be ascribed to molecules trapped near imperfections in the polycrystalline solid. Moreover, this result is independent of excitation energy. The absence of direct cage exit in the crystalline solid is structural in its origin: there are no direct cage exit paths in the crystalline solid in which a head-on collision with a xenon atom can be avoided. This principle was most clearly demonstrated in recent molecular dynamics simulations of HI photodissociation in crystalline xenon.<sup>26</sup> There, it was found that even the cage exit of an H atom is never direct—the atom exits after rattling around in the cage for several picoseconds.<sup>26</sup> This is obviously not the case in the liquid phase—the solvent cage in the liquid is never complete.

With the above arguments in mind it is possible to interpret the more obvious features of the wavelength dependence of branching ratios in the liquid phase. There are two distinct ranges

in which the  $\text{I}^-/\text{Cl}^-$  ratio increases nearly exponentially with increasing excitation energy, the range between 365 and 330 nm (see Figure 4) and the range between 290 and 270 nm (see Figure 5). These ranges will have to be associated with the access of potentials that correlate with the production of  $\text{I}^- + \text{Cl}$  in which the deposited excess energy can be funneled as kinetic energy of the neutral Cl atom. The obvious potentials are those constructed from  $\text{Xe}^+(^2\text{P}_{3/2})$  and  $\text{ICl}^-(^2\Pi_{1/2}, ^2\Pi_{3/2})$  in which the  $\text{ICl}^-$  coordinates are strictly repulsive and lead to the correct asymptotes, namely,  $\text{I}^-(^1\text{S}_0) + \text{Cl}(^2\text{P}_{3/2}, ^2\text{P}_{1/2})$ . These potential surfaces are well characterized,<sup>27</sup> and their correlations have been previously discussed in the context of both classical harpoon reactions ( $\text{ICl} + \text{alkali atoms}$ )<sup>28</sup> and harpoon reactions involving electronically excited rare-gas atoms.<sup>29</sup> The same considerations seem to be applicable in the present case even though one would expect a considerable modification of these ionic potentials due to solvation in the polarizable medium. Thus we tentatively ascribe the observed thresholds in the increase of branching ratios at 365 and 285 nm, to the opening of  $\text{Xe}^+(^2\text{P}_{3/2})\text{:ICl}^-(^2\Pi_{3/2})$  and  $\text{Xe}^+(^2\text{P}_{3/2})\text{:ICl}^-(^2\Pi_{1/2})$  product channels. Note that while the antibonding excess electron in  $\text{ICl}^-$  is localized on the I atom, the lowest energy surface for the charge-transfer complex,  $\text{Xe}^+(\text{ICl})^-$ , is that of  $\text{Xe}^+(^2\text{P}_{3/2})\text{:ICl}^-(^2\Sigma^+)$ , which correlates with  $\text{Cl}^-(^1\text{S}_0) + \text{I}(^2\text{P}_{3/2})$ . Thus near the excitation threshold only  $\text{Xe}_2^+\text{Cl}^-$  is to be expected, and this indeed is the observation—at 365 nm the  $\text{Xe}_2^+\text{I}^-$  emission is barely visible. It is important to note that the  $\text{ICl}^-(^2\Sigma^+)$  is deeply bound and that the vertical electron transfer to ICl near its energetic threshold could lead to a charge-transfer complex that would further be stabilized by the solvent. This nondissociative channel would not be observed in our experiments in which fluorescence from only the reactive channels are monitored. Charge-transfer thresholds are more directly obtained from absorption spectra. Such spectra have already been reported for homonuclear halogens in liquid xenon.<sup>6</sup> In all cases an absorption edge near 200 nm is observed and rationalized by simple solvation models. Given the similarity in vertical electron affinities of ICl and  $\text{Cl}_2$ , it is reasonable to expect a similar threshold in the present case, i.e., a two-photon threshold near  $\sim 400$  nm, which is in good agreement with the presented data. In the spectral range between 280 and 320 nm, where the  $\text{I}^-/\text{Cl}^-$  ratio is nearly constant, a distinct exit channel that can be ascribed to the predominance of certain molecular potentials cannot be identified.

**Entrance Channel and Optical Resonances.** There are several two-photon optical resonances that can lead to harpooning in these dense media. The first is that of two-photon excitation of ICl and subsequent electron hop:



The one-photon version of this process has been recently characterized in the gas phase by Donovan and co-workers using synchrotron radiation.<sup>30</sup> The optical resonance is with the Rydberg states of ICl, which act as a relay in populating the molecular ion-pair states. The latter are reactive with respect to collisions with xenon and efficiently produce the xenon halide exciplexes. It is not clear whether the ion-pair states of ICl participate in the liquid-phase reactions; however, the observed excitation cross sections for both iodide and chloride are loosely reminiscent of those observed in the gas phase in the 160–190 nm spectral range. The similarities include a small peak in the excitation spectrum of the iodide at 172 nm, a valley at 170 nm, and a maximum at 165 nm. All of these features can be discerned in our two-photon spectrum of Figure 4 (a small peak at 345 nm, a valley at 342 nm, and a peak near 330 nm). The similarity is

(27) Tasker, P. W.; Balint-Kurti, G.; Dixon, R. N. *Mol. Phys.* **1976**, *32*, 1651.

(28) Kwei, G. H.; Herschbach, D. R. *J. Chem. Phys.* **1969**, *51*, 1742.

(29) Kolts, J. H.; Velazco, J. E.; Setser, D. W. *J. Chem. Phys.* **1979**, *71*, 1247.

(30) Wilkinson, J. P. T.; Kerr, E. A.; Lawley, K. P.; Donovan, R. J.; Shaw, D.; Hopkirk, A.; Munro, I. *Chem. Phys. Lett.* **1986**, *130*, 213.

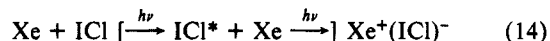
(26) Alimi, R.; Gerber, R. B.; Apkarian, V. A. *J. Chem. Phys.* **1988**, *89*, 174.

poorer in the case of the chloride action spectra. In the synchrotron experiments a pronounced valley at 169 nm flanked by maxima at 173 and 166 nm is observed. The latter feature is absent in our two-photon spectra. However, the similarities end there. In particular, the broad maximum in the excitation spectrum of the chloride at 355 nm is not observed in the gas phase. The range of excitations illustrated in Figure 5 has not been studied in the gas phase.

The direct two-photon-induced intermolecular charge transfer



is essential to explain the broad excitation resonances, the equivalents of which could not be expected in low-pressure gas-phase experiments. As in any two-photon transition, enhancement by intermediate-state resonances should be considered. Thus the coherent two-photon, two-electron excitation mechanism can be explicitly considered as



in which one photon is resonant with a molecular ICl transition (the promotion of a bonding electron to an antibonding state), and the second induces the charge transfer from Xe to the ICl\* intermediate. As mentioned above, in the spectral range of these studies, ICl contains several dissociative continua. Therefore the resonance condition for the first photon is always fulfilled. Then from the dissociative intermediate state, I $\cdots$ Cl, two resonances can be expected: charge transfer to the I end of the molecule or to the Cl end. The excitation maxima of these resonances should then correspond to the condensed-phase XeI(B $\leftarrow$ X) and XeCl(B $\leftarrow$ X) absorptions, which can be directly observed in xenon matrices doped with the atomic halogens. The diatomic charge-transfer excitation maxima are 270 and 355 nm for I- and Cl-doped matrices, respectively.<sup>3</sup> These expectations are then in good agreement with the observed excitation spectra: at 355 nm the chloride production efficiency peaks while the iodide is in constant decline, and toward the short-wavelength limit of the studies, near 260 nm, the iodide excitation peaks. As expected, the broad resonance at 355 nm is also observed in Cl<sub>2</sub>/Xe solutions.<sup>5</sup> There, extensive power-dependence studies of emission and transmission were performed to establish the cooperative nature of this transition—a coherent two-photon, two-electron transition.<sup>5</sup> This type of two-photon charge transfer, resonantly enhanced by a dissociative intermediate state, has also been most convincingly demonstrated in the molecular beam experiments of Xe:Cl<sub>2</sub> clusters.<sup>16</sup>

## Conclusions

Harpoon reactions have played a major role in the advancement of concepts in gas-phase molecular dynamics. Photoinduced harpoon reactions of rare-gas atoms with halogens, all variants of which have been well studied in the gas phase,<sup>31</sup> can be expected

to play a similar role in the case of molecular dynamics in condensed media. This, we hope, has been convincingly demonstrated in the present article in which we have demonstrated a powerful handle on such classic condensed-phase concepts as the cage effect and cage escape dynamics and clustering (solvent relaxation) and its dynamical consequences—the shielding from back reactions. Moreover these optically driven reactions offer a control on the reaction entrance channel, a control absent in classic harpoon reactions. As a result significant selectivity of reactions can be exercised.

In the specific case of ICl in Xe we have demonstrated efficient two-photon-induced harpooning occurs in a broad spectral range in the UV. The process can be enhanced by a two-photon resonance in which one photon promotes an ICl electron and the second promotes the harpoon electron. This allows a selectivity in the entrance channel—a choice between I or Cl as the primary electron acceptor. On the basis of branching ratios, at least two potential surfaces can be identified in the exit channel that lead to the production of I<sup>-</sup> + Cl with sudden cage exit on the Cl atom. These are assigned to the Xe<sup>+</sup>:ICl<sup>-</sup>( $\Pi_{3/2}$ ,  $\Pi_{1/2}$ ) surfaces. In the liquid phase, the sudden cage exit of the Cl atom is followed by a cage collapse by clustering of the polarizable solvent atoms around the newly created dipolar exciplex. The cage shields the iodide exciplex from back reaction with the geminately created Cl atom. The situation is quite different in the case of crystalline solids; there, direct cage exit is absent, and hence the predominant product is always the lowest energy channel, namely, the production of the chloride.

The experimental studies reported in the present article have relied strictly on fluorescence detection. Therefore, only the light-emitting reaction channels are monitored. The characterization of dark channels, such as the production of charge-transfer complexes of the molecular halogen ions, will be necessary to complete the overall dynamics. Transient absorption techniques are presently being implemented to achieve this end and to obtain absolute cross sections for the processes described in this report. A major impediment to a more rigorous development of these studies remains in our lack of understanding of many-body potentials, in particular ionic potentials in condensed media in which charge delocalization can be expected to play a significant role. Although in the case of these model systems, the molecular two-body potentials have served as useful references, more rigorous constructs will be essential for significant progress to occur.

*Acknowledgment.* This research is funded by the United States Air Force Astronautics Laboratory under Contract F04611-87-K-0024.

*Registry No.* ICl, 7790-99-0; Xe, 7440-63-3; Cl, 22537-15-1.

(31) Donovan, R. J.; Greenhill, P.; MacDonald, M. A.; Yench, A. J.; Hartree, W. S.; Johnson, K.; Jouvet, C.; Kuaran, A.; Simons, J. P. *Faraday Discuss. Chem. Soc.* **1987**, *84*, 12, and references therein.